

# Resummation and NLO matching of event shapes with effective field theory

Matthew D. Schwartz

*Johns Hopkins University, Baltimore, Maryland, USA*

(Received 28 September 2007; published 24 January 2008)

The resummed differential thrust rate in  $e^+e^-$  annihilation is calculated using soft-collinear effective theory (SCET). The resulting distribution in the two-jet region ( $T \sim 1$ ) is found to agree with the corresponding expression derived by the standard approach. A matching procedure to account for finite corrections at  $T < 1$  is then described. There are two important advantages of the SCET approach. First, SCET manifests a dynamical seesaw scale  $q = p^2/Q$  in addition to the center-of-mass energy  $Q$  and the jet mass scale  $p \sim Q\sqrt{1-T}$ . Thus, the resummation of logs of  $p/q$  can be cleanly distinguished from the resummation of logs of  $Q/p$ . Second, finite parts of loop amplitudes appear in specific places in the perturbative distribution: in the matching to the hard function, at the scale  $Q$ , in matching to the jet function, at the scale  $p$ , and in matching to the soft function, at the scale  $q$ . This allows for a consistent merger of fixed order corrections and resummation. In particular, the total NLO  $e^+e^-$  cross section is reproduced from these finite parts without having to perform additional infrared regulation.

DOI: [10.1103/PhysRevD.77.014026](https://doi.org/10.1103/PhysRevD.77.014026)

PACS numbers: 12.38.Cy, 12.39.Hg

## I. INTRODUCTION

Quantum chromodynamics is a perturbative field theory for  $\alpha_s < 1$ , corresponding to energies above  $\Lambda_{\text{QCD}} \sim 500$  MeV. However, setting up a good perturbation expansion is more difficult than simply working order by order in  $\alpha_s$ . The difficulty is that when computing a quantity with more than one scale, logarithms of ratios of those scales appear which invalidate the naive perturbation expansion. For example, in  $e^+e^-$  collisions at center-of-mass energy  $Q$ , we might look for the distribution of jets as a function of the invariant mass  $p^2$  of the jet. Then the differential cross section will have a correction of the form  $\alpha_s \log^2 \frac{p^2}{Q^2}$ . Even for  $\alpha_s < 1$  these large logarithms can dominate if  $p^2$  is sufficiently small. Luckily, these logarithms appear only in certain combinations even at higher order, so that all the terms of the form  $(\alpha_s \log^2 \frac{p^2}{Q^2})^n$  can be (re)summed at once. However, understanding which terms will appear, how to resum them, and how to combine the resummed result with fixed order results can be quite complicated. It is the goal of this paper to show how it can be done using effective field theory techniques.

In this paper, resummation and matching of event shapes are studied using soft-collinear effective theory (SCET) [1–5]. Event shapes are observables which are sensitive to the overall distribution of final state particles, and therefore involve both short and long distance physics. We will consider mainly the event shape  $\tau = 1 - T$  where the thrust  $T$  is defined by

$$T = \max_{\mathbf{n}} \frac{\sum_i |\mathbf{p}_i \cdot \mathbf{n}|}{\sum_i |\mathbf{p}_i|} \quad (1)$$

summing over all momentum 3-vectors  $\mathbf{p}_i$  in the event and maximizing over unit 3-vectors  $\mathbf{n}$ . In the threshold region near  $\tau = 0$  large logarithms of the form  $\alpha_s \log^2 \tau$  appear at

fixed order in perturbation theory. The resummed result will be valid even if  $\alpha_s \log^2 \tau$  is large, as long as  $\alpha_s$  and  $\alpha_s \log \tau$  are small.

Effective field theories provide a systematic approach to resummation. They separate out physics at a hard underlying scale  $Q$  from physics associated with a scale of interest  $p^2 \sim Q^2 \tau$  and from even lower scales. At each scale a separate matching calculation is done which is independent of physics at asymptotically lower or higher energy. Then the scale dependence is calculated using the renormalization group. In this way, large logarithms cannot appear because no two largely separated scales are accessible to the theory at the same time. The soft-collinear effective theory works by separating the degrees of freedom of QCD into soft modes and collinear modes in different directions. The relevant scales are then associated with the observable of interest, such as  $Q^2 \tau$ , or with the large components of the collinear modes.

The resummation of event shapes in  $e^+e^-$  is not currently of extreme importance phenomenologically. It nevertheless provides a clean arena (as compared to hadron collisions) to explore resummation and matching. The SCET techniques and most of the formulas we discuss here were originally developed for  $B$ -physics, such as resummation in  $b \rightarrow s\gamma$  decays [1,6–8]. They have also been applied to the study of deep-inelastic-scattering near  $x = 1$  [9–11] and to the production of massive jets initiated by top quark decays [12]. One convenient feature of effective field theories is factorization, which allows us to use objects, such as soft and jet functions, calculated in one process to study another. Thus, most of the hard work required for calculation of the distributions we describe here can be extracted from the literature. Nevertheless, there are certain features, in particular, the NLO matching step, for which event shapes are uniquely illuminating.

The breakdown of naive perturbation theory due to the appearance of large logarithms is independent of  $\alpha_s$  blow-

ing up and of nonperturbative effects. To emphasize this point, and to simplify the resummed expressions, the running of  $\alpha_s$  will be simply turned off (setting  $\beta = 0$ ) for most of this paper. Working in the conformal limit removes one scale ( $\Lambda_{\text{QCD}}$ ) from the problem and thus clarifies which large logs are being resummed. It is not hard to turn  $\beta$  back on, as will be shown in Sec. V. Also, we will be including all one-loop results but no two-loop results. Thus, our expressions will not contain a complete next-to-leading log resummation, which should also resum the two-loop double logs.

There are three steps involved in the calculation of event shapes in SCET, associated with three separate scales. At the hard scale  $\mu_h \sim Q$ , QCD is matched onto SCET by demanding parton level matrix elements in the two theories be the same. This can be done at leading order by matching onto an operator  $\mathcal{O}_2$  with two collinear fields, or at next-to-leading order by matching in addition to an operator  $\mathcal{O}_3$  with collinear fields in three directions [13,14]. The threshold resummation only involves  $\mathcal{O}_2$  as the matrix elements of  $\mathcal{O}_3$  vanish near  $\tau = 0$ . (An alternative approach to  $\mathcal{O}_3$  matching is described in [15].) At the scale  $\mu_j \sim Q\sqrt{\tau}$ , the collinear fields freeze and can be removed from the theory by integrating them out. This results in the jet function  $J(p^2)$ . Finally, even though we are interested in a distribution at the scale  $Q\sqrt{\tau}$ , the soft degrees of freedom remain relevant down to a scale  $\mu_s = Q\tau$ , after which they too can be integrated out of the theory. The fixed order result will have large logarithms of  $\mu_h/\mu_j$  and  $\mu_j/\mu_s$ , but in the resummed result all these logs are exponentiated and innocuous.

Before we present the factorization formula and calculate the thrust distribution in SCET, we will review the way resummation of thrust is traditionally handled. There are a number of ways to resum event shapes [16–22]. Since the focus of this work is on comparisons to SCET, we will confine our attention to the original approach of Catani, Trentadue, Turnock, and Webber [16] (which will be referred to as CTTW throughout). Moreover, most of the other approaches reduce to [16] at next-to-leading fixed order in  $\alpha_s$  (NLO) and to leading log, so no significant loss of generality is sustained. We will find that in the two-jet limit SCET also agrees with CTTW to the order we are working, although the resummed expressions are not exactly the same.

A more significant difference is in the NLO matching. A critical advantage of the effective theory approach is that the finite parts of loop amplitudes are automatically incorporated into the perturbative expressions. For example, the total NLO cross section for  $e^+e^-$  is reproduced by combining the finite parts of the hard, jet, and soft functions and a contribution from a finite integral over higher-order operators in SCET. This does not necessarily entail less work than in calculating the total cross section through the traditional combination of real and virtual contributions.

However, due to factorization, the infrared divergent contributions which are absorbed into the jet and soft functions are universal and thus they could potentially be used for many processes.

## II. PERTURBATIVE QCD

In this section, we will review some basic results from QCD on thrust, and the resummed expressions presented in [16].

To begin, consider the parton model description of  $e^+e^-$  annihilation. At order  $\alpha_s^0$ , the only process which contributes is  $e^+e^- \rightarrow \bar{q}q$ . These two jets have no structure and hence the cross section is simply  $d\sigma/d\tau = \sigma_0\delta(\tau)$ , where  $\sigma_0$  is leading order total  $e^+e^-$  annihilation cross section.

At order  $\alpha_s^1$ , there are two  $e^+e^- \rightarrow \bar{q}qg$  diagrams which contribute

$$d\sigma_{\text{parton}} \sim \left| \begin{array}{c} \text{diagram 1} \\ + \\ \text{diagram 2} \end{array} \right|^2, \quad (2)$$

where the photon line on the bottom is the  $e^+\gamma^\mu e^-$  current coming in. The differential cross section is

$$\left[ \frac{1}{\sigma_0} \frac{d^2\sigma}{dsdt} \right]_{\text{parton}} = \delta(s)\delta(t) + \bar{\alpha} \frac{s^2 + t^2 + 2u}{st} \quad (3)$$

where we have defined

$$\bar{\alpha} \equiv \frac{2\alpha_s}{3\pi} \quad (4)$$

and the reduced Mandelstam variables are  $s = (p_g + p_q)^2/Q^2$  and  $t = (p_g + p_{\bar{q}})^2/Q^2$  with  $s + t + u = 1$ .

Now, for 3-parton events the thrust variable  $\tau = 1 - T$  reduces to

$$\tau = \min(s, t, u). \quad (5)$$

So that

$$\left[ \frac{1}{\sigma_0} \frac{d\sigma}{d\tau} \right]_{\text{parton}} = \delta(\tau) + \bar{\alpha} \left[ \frac{2(3\tau^2 - 3\tau + 2)}{\tau(1-\tau)} \log \frac{1-2\tau}{\tau} - \frac{3(1-3\tau)(1+\tau)}{\tau} \right] \quad (6)$$

$$= \delta(\tau) + \bar{\alpha} \left[ \frac{-4\log\tau - 3}{\tau} \right] + \bar{\alpha} d_{\text{fin}}(\tau). \quad (7)$$

The second line is written to manifest the singularity structure. The remainder  $d_{\text{fin}}(\tau)$  is finite as  $\tau \rightarrow 0$ .

Instead of the differential thrust distribution, it is useful to work directly with the integrated quantity

$$R(\tau) = \int_0^\tau \frac{d\sigma}{d\tau'} d\tau'. \quad (8)$$

For small  $\tau$ ,

$$R_{\text{parton}}(\tau) \sim -2\bar{\alpha}\log^2\tau - 3\bar{\alpha}\log\tau. \quad (9)$$

Here we see explicitly the large logarithms  $\alpha_s\log^2\tau$  and  $\alpha_s\log\tau$  which demand resummation.

A useful theoretical trick, used in [16] and in [12], is to employ a hemisphere mass definition. This greatly simplifies the factorization formula in the two-jet limit. The hemisphere momentum  $p_L(p_R)$  is defined to be the sum of the 4-momenta of all the particles in the hemisphere of the left (right) jet. Then thrust reduces to  $\tau = (p_L^2 + p_R^2)/Q^2$ , and we can calculate it from

$$\frac{d\sigma}{d\tau} = \int \frac{d^2\sigma}{dp_L^2 dp_R^2} \delta\left(\tau - \frac{p_L^2 + p_R^2}{Q^2}\right), \quad (10)$$

which we will see has a closed form expression.

The traditional approach to resummation which we review here is due to Catani *et al.* [16]. The basic idea is that terms of the form  $(\bar{\alpha}\log^2\tau)^n$  come from multiple real collinear and soft emissions. The kinematics of multiple collinear emissions can be modeled by parton branchings, with branching probabilities proportional to the Altarelli-Parisi splitting functions

$$\frac{d^2\sigma^{n+1}}{dtdz} = d\sigma^n \times P_{qq} = d\sigma^n \times \bar{\alpha} \frac{1+z^2}{t(1-z)}. \quad (11)$$

In the two-jet limit, the corrections due to soft effects can be modeled by imposing angular ordering. All of this follows from the coherent-branching algorithm developed in [23]. In fact, more general methods are available for handling soft emissions (for example, [24]). But, to NLO for event shapes like thrust, the methods set up in [16] are sufficient to compare to SCET.

In the two-jet limit, the factorized expression for the differential cross section in CTTW is

$$\left[\frac{1}{\sigma_0} \frac{d^2\sigma_2}{dp_L^2 dp_R^2}\right]_{\text{CTTW}} = J_C(Q^2, p_L^2) J_C(Q^2, p_R^2). \quad (12)$$

The subscript on  $\sigma_2$  refers to the 2-jet contribution.  $J_C$  has a simple physical interpretation: it is the probability of finding a final state jet with invariant mass  $p^2$ . Thus, it satisfies

$$\int_0^\infty dp^2 J_C(Q^2, p^2) = 1. \quad (13)$$

$Q$  is a scale associated with the hard process. We will see later that the equivalent jet function in SCET has a different normalization.

At leading order the jet is a massless parton and so  $J_C(Q^2, p^2) = \delta(p^2)$ . At next-to-leading order, the coherent branching algorithm allows one-angular ordered emission. So

$$J_C(Q^2, p^2) = \delta(p^2) + \bar{\alpha} \int_0^{Q^2} \frac{d\tilde{q}^2}{\tilde{q}^2} \int_0^1 dz \frac{1+z^2}{1-z} \times \delta(p^2 - z(1-z)\tilde{q}^2) + \dots. \quad (14)$$

Here  $z$  is the energy fraction in the emission and  $\tilde{q}^2 = \frac{p^2}{z(1-z)} \approx E^2(1 - \cos\theta)$ . The angular ordering constraint for the coherence of soft emissions is implicit in the restriction  $\tilde{q} < Q$ ; for  $p^2 > 0$  it cuts off the infrared divergences in the integral as  $z \rightarrow 1$ . Evaluating (14) gives

$$J_C(Q^2, p^2) = \delta(p^2) + \bar{\alpha} \left[ \frac{-2\log\frac{p^2}{Q^2} - \frac{3}{2}}{p^2} \right]_{\star}^{[p^2, Q^2]} + \dots. \quad (15)$$

Thus, to first order in  $\alpha_s$ ,

$$\left[ \frac{1}{\sigma_0} \frac{d\sigma_2}{d\tau} \right]_{\text{CTTW}} = \delta(\tau) + \bar{\alpha} \left[ \frac{-4\log\tau - 3}{\tau} \right]_{\star}^{[\tau, 1]}, \quad (16)$$

which reproduces the divergent as  $\tau \rightarrow 0$  part of the parton model result (7).

Here we have introduced the  $\star$  distribution (alternatively called the  $R$ - or  $\mu$ -distribution), which is a generalization of the  $+$ -distribution. It is uniquely defined by the two conditions

$$[f(x)]_{\star}^{[x, a]} = f(x) \quad \text{for } x > 0 \quad (17)$$

$$\int_0^a dx [f(x)]_{\star}^{[x, a]} g(x) = \int_0^a dx f(x) [g(x) - g(0)] \quad (18)$$

For clarity, we have added to the notation an explicit instance of the dependent variable  $x$  in  $[f]_{\star}^{[x, a]}$ . A useful relation is

$$[f(x)]_{\star}^{[x, a]} = [f(x)]_{\star}^{[x, b]} + \delta(x) \int_a^b dx' f(x'). \quad (19)$$

This will be used extensively in the next section.

The leading order resummation is performed by iterating the angular-ordered emissions. This leads to an integro-differential equation for  $J_C(Q^2, p^2)$ , similar to the evolution equation for parton-distribution functions. The equation is solved in an integrated form, and the resummed expression for the integrated thrust in the two-jet limit is

$$\left[ \frac{1}{\sigma_0} R_2(\tau) \right]_{\text{CTTW}} = \exp[-2\bar{\alpha}\log^2\tau - 3\bar{\alpha}\log\tau] \times \frac{e^{-2\gamma_E\eta}}{\Gamma[2\eta + 1]}, \quad (20)$$

where

$$\eta = -2\bar{\alpha}\log\tau. \quad (21)$$

This equation is a combination of expressions in [16] taken with  $\beta = 0$ . Expanding  $R_2'(\tau) = \frac{d\sigma_2}{d\tau}$  to order  $\alpha_s$  the fixed

order result (16) is reproduced. This expression is resummed in the sense that  $R'_2(\tau) \rightarrow 0$  as  $\tau \rightarrow 0$ , in contrast to the fixed order result (16) for  $d\sigma$  or the parton model expression (7) which diverge as  $\tau \rightarrow 0$ .

### III. SOFT-COLLINEAR EFFECTIVE THEORY

Having reviewed the way the resummed thrust distribution is traditionally calculated, we now turn to the equivalent calculation in SCET. We will see that there are a number of advantages of this effective field theory treatment. Instead of a classical treatment, where multiple real emissions are summed at the level of the cross section, the entire resummation is done in SCET through the renormalization group. This makes explicit the various scales in the problem, and allows greater freedom to choose those scales to minimize the large logarithms in the distributions of interest.

The idea behind SCET is to separate out the quarks and gluons of QCD into soft and collinear degrees of freedom. A collinear field is associated with a lightlike direction  $n^\mu$ . The component of its momentum in that direction,  $p^- = \bar{n} \cdot p$ , must be much larger than any of the other momentum components. All the QCD degrees of freedom which could change this momentum have been integrated out, so  $p^-$  appears as a fixed label. For example, a collinear quark is written as  $\xi_n(p)$  with a fixed  $p^-$ . In addition to collinear quarks and gluons, there are soft quarks and gluons. These soft fields can only interact with each other or transfer momentum to the soft components  $p^+ = n \cdot p$  of a collinear field.

The Lagrangian of SCET has a separate gauge invariance associated with soft gluons and gluons in each collinear direction. It is useful to maintain this gauge invariance explicitly in the operators of the theory with the use of Wilson lines. For example, a two-jet operator is

$$\mathcal{O}_2 = \bar{\xi}_{\bar{n}} W_{\bar{n}} Y_{\bar{n}} \gamma^\mu Y_n^\dagger W_n^\dagger \xi_n, \quad (22)$$

where

$$W_n(x) = P \exp \left\{ ig \int ds \bar{n} \cdot A_n(\bar{n}s + x) \right\} \quad (23)$$

$$Y_n(x) = P \exp \left\{ ig \int ds n \cdot A_s(ns + x) \right\}. \quad (24)$$

The collinear Wilson lines  $W_n$  maintain collinear gauge invariance and the soft Wilson lines  $Y_n$  maintain soft gauge invariance.

The starting point in the effective theory approach to event shapes is again factorization in the two-jet limit. In SCET, the event-shape distributions near the endpoint come from matrix elements of  $\mathcal{O}_2$  [12,14,25,26]. In terms of the hemisphere masses  $p_L$  and  $p_R$  defined above, factorization implies [12]

ization implies [12]

$$\left[ \frac{d^2 \sigma_2}{dp_L^2 dp_R^2} \right]_{\text{SCET}} = |C_H(\mu)|^2 \int dk_L dk_R J(p_L^2 - Qk_L, \mu) \times J(p_R^2 - Qk_R, \mu) S(k_L, k_R, \mu). \quad (25)$$

The hard function  $C_H(\mu)$ , the jet functions  $J(p^2, \mu)$ , and the soft function  $S(k, \mu)$  will be defined below.

The form of this factorized expression (25) has a physical explanation. Each jet function  $J(p^2, \mu)$  comes from one of the collinear quarks. It represents, like  $J_C$ , the probability for producing a jet of invariant mass  $p^2$  from that collinear field (the precise relation to  $J_C$  is explored below). Recall that the large component of the momentum of a collinear field  $p^- = \bar{n} \cdot p$  is fixed. Since, in the two-jet limit, the jets are back to back with center-of-mass energy  $Q$ , we must have  $p^- \sim Q$ . The small component  $p^+ = n \cdot p$  can vary. If there are no soft effects, then the hemisphere mass is simply  $p_H^2 = p^2 = p^- p^+$ . However, as the factorization formula implies, the collinear jet can give up some soft momentum to the soft QCD background, leading to  $p^+ \rightarrow p^+ - k$ . The hemisphere mass is unchanged by this emission, but now  $p^2 = p^-(p^+ - k) = p_H^2 - Qk$ , which explains the form of (25).

The function  $C_H$  is a hard function, which comes from integrating out hard modes of QCD in matching to SCET. Demanding

$$\langle \bar{q} \gamma^\mu q \rangle = C_H \langle \xi_n \gamma^\mu \xi_{\bar{n}} \rangle \quad (26)$$

for states with two external quarks lets us calculate  $C_H$  order by order in perturbation theory. The computation entails taking the difference between QCD and SCET graphs, such as

$$C_H \sim \text{[QCD graph]} - \text{[SCET graph]}, \quad (27)$$

where the  $\otimes$  refers to an insertion of  $\mathcal{O}_2$ , and the right diagram is only a representative contribution (for details, see [13]). The difference is finite because the infrared divergences in QCD and SCET are the same and the UV divergences are removed with counterterms. At one-loop the matching gives [9,13]

$$C_H(\mu) = 1 + c_H + \frac{\Gamma_H}{2} \log^2 \frac{\mu^2}{Q^2} - \gamma_H \log \frac{\mu^2}{Q^2}, \quad (28)$$

with  $c_H = \bar{\alpha}(-4 + \frac{7\pi^2}{12} - \frac{3\pi}{2}i)$ ,  $\Gamma_H = -\bar{\alpha}$ , and  $\gamma_H = \frac{3}{2}\bar{\alpha}$ .

The anomalous dimension and renormalization group evolution of  $C_H(\mu)$  can be found from the UV divergences of the same 1-loop graphs. The RG equation is

$$\frac{dC_H(\mu)}{d \log \mu} = \left( -2\Gamma_H \log \frac{Q^2}{\mu^2} - 2\gamma_H \right) C_H(\mu), \quad (29)$$



with solution

$$C_H(\mu) = C_H(\mu_h) \exp\left[\frac{\Gamma_H}{2} \log^2 \frac{\mu^2}{\mu_h^2} - \gamma_H \log \frac{\mu^2}{\mu_h^2}\right] \times \left(\frac{Q^2}{\mu_h^2}\right)^{-\Gamma_H \log(\mu^2/\mu_h^2)}. \quad (30)$$

To first order in  $\alpha_s$ , the  $\mu_h$  dependence drops out and (28) is reproduced. The natural matching scale  $\mu_h = Q$  is manifest in this expression.

The jet function  $J(p^2, \mu)$  is the imaginary part of the propagator of a collinear quark. It is defined by [12,27]

$$J(p^2, \mu) \sim \text{Disc} \left\{ \begin{array}{c} \text{---} \otimes \text{---} \text{---} \otimes \text{---} \\ \text{---} \otimes \text{---} \text{---} \otimes \text{---} \\ \text{---} \otimes \text{---} \text{---} \otimes \text{---} \\ \vdots \end{array} \right\}. \quad (32)$$

Some of the infrared divergences in these graphs are cut off because the collinear quark is taken to have invariant mass  $p^2$ . These calculations have been done in the context of  $b \rightarrow s\gamma$  [6,7] and for deep-inelastic scattering [9,11] and the jet function is known to two loops [27]. Because of factorization, the same jet function applies in these processes and in  $e^+e^-$  annihilation. To first order in  $\alpha_s$ , the result is

$$J(p^2, \mu) = \delta(p^2)[1 + c_J] + \left[\frac{\Gamma_J \log \frac{p^2}{\mu^2} + \gamma_J}{p^2}\right]_{\star}^{[p^2, \mu^2]}, \quad (33)$$

with  $c_J = \bar{\alpha}(\frac{7}{2} - \frac{\pi^2}{2})$ ,  $\Gamma_J = 2\bar{\alpha}$ , and  $\gamma_J = -\frac{3}{2}\bar{\alpha}$ .

The renormalization group evolution of the jet function, in contrast to that of the hard function, is nonlocal in  $p^2$

$$\frac{dJ(p^2, \mu)}{d \log \mu} = \left[-2\Gamma_J \log \frac{p^2}{\mu^2} - 2\gamma_J\right] J(p^2, \mu) + 2\Gamma_J \int_0^{p^2} dq^2 \frac{J(p^2, \mu) - J(q^2, \mu)}{p^2 - q^2}. \quad (34)$$

This is similar to the Altarelli-Parisi equation for the evolution of the parton distribution functions (pdfs). In contrast to pdfs, however, the jet function  $J(p^2, \mu)$  is perturbative as long as  $p^2 > \Lambda_{\text{QCD}}$ . Simplification is achieved through use of the Laplace transform [11],

$$\tilde{j}(\nu) = \int dp^2 e^{-\nu p^2} J(p^2, \mu), \quad (35)$$

whereby the evolution becomes local in  $\nu$

$$\frac{d\tilde{j}(\nu, \mu)}{d \log \mu} = \left(-2\Gamma_J \log \frac{1}{\mu^2 \nu e^{\gamma_E}} - 2\gamma_J\right) \tilde{j}(\nu, \mu). \quad (36)$$

Now the RGE can be solved like that of  $C_H$ :

$$J(p^2, \mu) = -\frac{1}{\pi(\bar{n} \cdot p)} \times \text{Im} \left[ \int d^4 x e^{-ipx} \langle T \{ (\bar{\xi}_{\bar{n}} W_{\bar{n}}^\dagger)(0) \not{n} (W_n \xi_n)(x) \} \rangle \right]. \quad (31)$$

It can be thought of as the spectral density for a jet of collimated particles interacting with a soft QCD background. The jet function can be calculated order-by-order in perturbation theory through the discontinuity of conventional Feynman diagrams, such as

$$\tilde{j}(\nu, \mu) = \exp\left[\frac{\Gamma_J}{2} \log^2 \frac{\mu^2}{\mu_j^2} - \gamma_J \log \frac{\mu^2}{\mu_j^2}\right] \times (\nu e^{\gamma_E} \mu_j^2)^{-\eta_j} \tilde{j}(\nu, \mu_j) \quad (37)$$

with

$$\eta_j = -\Gamma_J \log \frac{\mu^2}{\mu_j^2}. \quad (38)$$

Finally, the inverse Laplace transform produces [11]

$$J(p^2, \mu) = \exp\left[\frac{\Gamma_J}{2} \log^2 \frac{\mu^2}{\mu_j^2} - \gamma_J \log \frac{\mu^2}{\mu_j^2}\right] \tilde{j}(\partial_{\eta_j}) \times \left[\frac{1}{p^2} \left(\frac{p^2}{\mu_j^2}\right)^{\eta_j}\right]_{\star}^{[p^2, \mu_j^2]} \frac{e^{-\gamma_E \eta_j}}{\Gamma[\eta_j]}, \quad (39)$$

where

$$\tilde{j}(\partial_{\eta_j}) = 1 + c_J + \Gamma_J \frac{\pi^2}{12} + \frac{\Gamma_J}{2} \partial_{\eta_j}^2 + \gamma_J \partial_{\eta_j}. \quad (40)$$

The functional dependence on  $\partial_{\eta_j}$  in  $\tilde{j}(\partial_{\eta_j})$  comes from a functional dependence on  $\log \frac{p^2}{\mu^2}$  in the fixed order expression for the jet function (33) at the matching scale  $\mu = \mu_j$ .

Finally, we have to calculate the soft function  $S(k_L, k_R, \mu)$ . It is defined through matrix elements of soft Wilson lines [12,28]

$$S(k_L, k_R, \mu) = \sum_X \langle 0 | Y_{\bar{n}}^* Y_n | X \rangle \langle X | Y_n^\dagger Y_{\bar{n}}^\dagger | 0 \rangle. \quad (41)$$

Unlike the jet function, the soft function is often evaluated at scales  $k \sim \Lambda_{\text{QCD}}$ , where it is nonperturbative. It can, in principle, be measured experimentally and then be evolved perturbatively, like the pdfs. Or it can be modeled [12,29,30]. However, in our case, since we are taking  $\alpha_s$  to be small and fixed, it can be calculated in perturbation theory. Even if  $S$  is nonperturbative, the perturbative cal-

ulation is useful because the UV divergences dictate the anomalous dimensions and hence the evolution equation.

The soft function, being completely defined in terms of Wilson lines, can be calculated in QCD through diagrams such as

$$S(k_L, k_R, \mu) \sim \text{diagram 1} + \text{diagram 2} + \text{diagram 3} + \dots, \quad (42)$$

where the kinked lines are Wilson lines in the  $n$  and  $\bar{n}$  directions. To order  $\alpha_s$ ,  $S(k_L, k_R)$  can be written as a product

$$S(k_L, k_R, \mu) = S(k_L, \mu)S(k_R, \mu) \quad (43)$$

where [28]

$$S(k, \mu) = \delta(k)[1 + c_S] + \left[ \frac{\Gamma_S \log \frac{k}{\mu} + \gamma_S}{k} \right]_{\star}^{[k, \mu]}, \quad (44)$$

with  $c_S = \bar{\alpha} \frac{\pi^2}{12}$ ,  $\Gamma_S = -4\bar{\alpha}$ , and  $\gamma_S = 0$ .

The evolution of the soft function involves the same kind of nonlocal equation as for the jet function. This can be seen from examining its anomalous dimension directly, or from RG invariance of the convolution appearing in the factorization formula (25). The solution is therefore similar. Explicitly,

$$S(k, \mu) = \exp \left[ \frac{\Gamma_S}{2} \log^2 \frac{\mu}{\mu_s} - \gamma_S \log \frac{\mu}{\mu_s} \right] \tilde{s}(\partial_{\eta_s}) \times \left[ \frac{1}{k} \left( \frac{k}{\mu_s} \right)^{\eta_s} \right]_{\star}^{[k, \mu_s]} \frac{e^{-\gamma_E \eta_s}}{\Gamma[\eta_s]}, \quad (45)$$

where

$$\tilde{s}(\partial_{\eta_s}) = 1 + c_S + \Gamma_S \frac{\pi^2}{12} + \frac{\Gamma_S}{2} \partial_{\eta_s}^2 + \gamma_S \partial_{\eta_s} \quad (46)$$

and

$$\eta_s = -\Gamma_S \log \frac{\mu}{\mu_s}. \quad (47)$$

Expanding to first order in  $\alpha_s$  reproduces (44).

Now we have all the ingredients appearing in the factorization formula (25). At order  $\alpha_s$ , the result is

$$\left[ \frac{1}{\sigma_0} \frac{d^2 \sigma_2}{dp_L^2 dp_R^2} \right]_{\text{SCET}} = \delta(p_L^2) \delta(p_R^2) \left[ 1 + \bar{\alpha} \left( -1 + \frac{\pi^2}{3} \right) \right] + \bar{\alpha} \delta(p_R^2) \left[ \frac{2 \log \frac{Q^2}{p_L^2} - \frac{3}{2}}{p_L^2} \right]_{\star}^{[p_L^2, Q^2]} + \bar{\alpha} \delta(p_L^2) \left[ \frac{2 \log \frac{Q^2}{p_R^2} - \frac{3}{2}}{p_R^2} \right]_{\star}^{[p_R^2, Q^2]}. \quad (48)$$

Note that the dependence on all the scales  $\mu$ ,  $\mu_h$ ,  $\mu_j$ , and  $\mu_s$  has completely canceled. This is a nontrivial result which requires three relations among the six anomalous dimensions:

$$\Gamma_J + \frac{\Gamma_S}{2} = \Gamma_H + \Gamma_J + \frac{\Gamma_S}{4} = \gamma_H + \gamma_J + \frac{\gamma_S}{2} = 0 \quad (49)$$

and is a strong consistency check on the entire formalism.<sup>1</sup>

Already SCET can be compared to CTTW. The differential distribution in SCET, Eq. (48), matches the distribution in CTTW, Eq. (12), when the jet functions are expanded to first order using Eq. (15). The SCET expression has an additional finite piece (the  $-1 + \frac{\pi^2}{3}$  term) which comes from loop graphs which do not enter into the traditional formulation.

Still working at leading order in  $\alpha_s$ , SCET produces a simple form for the thrust distribution near  $\tau = 0$ :

$$\left[ \frac{1}{\sigma_0} \frac{d\sigma_2}{d\tau} \right]_{\text{SCET}} = \delta(\tau) \left[ 1 + \bar{\alpha} \left( -1 + \frac{\pi^2}{3} \right) \right] + \bar{\alpha} \left[ \frac{-4 \log \tau - 3}{\tau} \right]_{\star}^{[\tau, 1]}. \quad (50)$$

This reproduces the leading behavior for small  $\tau$  of the both the parton model expression, Eq. (7), and the resummed expression with the functions  $J_C$  expanded to first order, Eq. (16).

To get the resummed thrust distribution from SCET, we need to calculate a couple of convolution integrals. First, the soft and jet functions must be combined into

$$K(p^2, \mu) = \int dk J(p^2 - kQ, \mu) S(k, \mu). \quad (51)$$

Second, the  $K$  functions must be integrated against the event shape. For thrust, we need

$$R_2(\tau) = |C_H(\mu)|^2 \int K(p_L^2, \mu) K(p_R^2, \mu) \theta \left( \tau - \frac{p_L^2 + p_R^2}{Q^2} \right). \quad (52)$$

Both of these convolutions can be evaluated by performing the Laplace transform.

<sup>1</sup>The relations among the  $\Gamma$ s can be understood on more general grounds by relating the  $\Gamma$ s to a universal cusp anomalous dimension [31].

Note that the function names can be misleading. Here,  $C_H(\mu)K(p^2, \mu)$  [and not just the SCET jet function  $J(p^2, \mu)$ ] is playing the role of  $J_C(p^2)$  from the CTTW formulation. Thus, the CTTW jet function is a combination of the soft and jet functions in SCET, as expected because the coherent branching algorithm used to derive it incorporates both soft and collinear effects.

Solving the  $K$  function with the Laplace transform techniques gives

$$K(p^2, \mu) = \exp\left[\frac{\Gamma_J}{2}\log^2\frac{\mu^2}{\mu_j^2} - \gamma_J\log\frac{\mu^2}{\mu_j^2}\right] \times \exp\left[\frac{\Gamma_S}{2}\log^2\frac{\mu}{\mu_s} - \gamma_S\log\frac{\mu}{\mu_s}\right]\left(\frac{Q\mu_s}{\mu_j^2}\right)^{-\eta_s} \quad (53)$$

$$\times \left[\frac{\Gamma_S}{2}\log^2\frac{Q\mu_s}{\mu_j^2} - \Gamma_S\log\frac{Q\mu_s}{\mu_j^2}\partial_{\eta_k} + \tilde{k}(\partial_{\eta_k})\right] \times \left[\frac{1}{p^2}\left(\frac{p^2}{\mu_j^2}\right)^{\eta_k}\right]_{\star}^{[p^2, \mu_j^2]} \frac{e^{-\gamma_E\eta_k}}{\Gamma[\eta_k]}, \quad (54)$$

where

$$\left[\frac{1}{\sigma_0}R_2(\tau)\right]_{\text{SCET}} = |C_H(\mu_h)|^2 \exp\left[2\bar{\alpha}\log^2\frac{\mu_h^2}{\mu_j^2} + 3\bar{\alpha}\log\frac{\mu_h^2}{\mu_j^2} - \bar{\alpha}\log^2\frac{\mu_h^2}{\mu_s^2}\right]\left(\frac{Q\mu_s}{\mu_j^2}\right)^{-4\bar{\alpha}\log(\mu_h^2/\mu_s^2)} \times \left[-2\bar{\alpha}\log^2\frac{Q\mu_s}{\mu_j^2} + 4\bar{\alpha}\log\frac{Q\mu_s}{\mu_j^2}\partial_{2\eta_k} + \tilde{k}(\partial_{2\eta_k})\right]^2 \left(\frac{Q^2\tau}{\mu_j^2}\right)^{2\eta_k} \frac{e^{-2\gamma_E\eta_k}}{\Gamma[2\eta_k + 1]}. \quad (58)$$

Note that this expression is explicitly independent of  $\mu$ .

Now, choosing the natural scales  $\mu_h = Q$ ,  $\mu_j = Q\sqrt{\tau}$ , and  $\mu_s = \mu_j^2/Q = Q\tau$  to remove the large logs, the thrust distribution becomes

$$\left[\frac{1}{\sigma_0}R_2(\tau)\right]_{\text{SCET}} = \exp[-2\bar{\alpha}\log^2\tau - 3\bar{\alpha}\log\tau]\tilde{r}(\partial_\eta) \times \frac{e^{-2\gamma_E\eta}}{\Gamma[2\eta + 1]} \quad (59)$$

with

$$\tilde{r}(\partial_\eta) = 1 + \left(-1 + \frac{\pi^2}{3}\right)\bar{\alpha} - \frac{\pi^2}{3}\bar{\alpha} - \frac{1}{2}\bar{\alpha}\partial_\eta^2 - \frac{3}{2}\bar{\alpha}\partial_\eta \quad (60)$$

and  $\eta = -2\bar{\alpha}\log\tau$  as in Eq. (21).

This expression would be identical to the CTTW expression, Eq. (20), if  $\tilde{r} = 1$ . Recall that the function  $\tilde{r}$  comes from 1-loop matching in SCET, which turns into boundary conditions for the renormalization group evolution. In the approach of CTTW the boundary condition is simply that  $J_C(p^2) = \delta(p^2)$ . Nevertheless, the effect of  $\tilde{r} \neq 1$  to order  $\alpha_s$  is only to provide a finite constant, as

$$\tilde{k}(\partial_{\eta_k}) = 1 + c_J + c_S + \frac{\pi^2}{12}(\Gamma_J + \Gamma_S) + \left(\frac{\Gamma_J + \Gamma_S}{2}\right)\partial_{\eta_k}^2 + (\gamma_J + \gamma_S)\partial_{\eta_k} \quad (55)$$

and

$$\eta_k = \eta_s + \eta_j = 2\bar{\alpha}\log\frac{\mu_j^2}{\mu_s^2}. \quad (56)$$

Note the residual logarithms of  $Q\mu_s/\mu_j^2$  in line (54) which are not resummed. These imply that we cannot choose  $\mu_j = \mu_s$ . Instead, the natural scales (those which remove the large logs) should satisfy  $\mu_s = \mu_j^2/Q$ . Then, we can evolve either the jet function from  $\mu_j$  down to  $\mu_s$  or the soft function from  $\mu_s$  up to  $\mu_j$  but there is not a single scale which can minimize all the large logs.

Finally, to evaluate the convolution for the thrust integral, we use the Laplace transform of the  $\theta$ -function

$$\int_0^\infty dp^2\theta(p^2)e^{-\nu p^2} = \frac{1}{\nu}. \quad (57)$$

Combining this with the expression for  $K(p^2, \mu)$  above, the SCET prediction for thrust in the 2-jet limit is

can be seen from comparing Eqs. (16) and (50). That is, there is no contribution of order  $\eta$  in the difference, only of order  $\eta^2$  and higher. Beyond order  $\alpha_s$ , the  $\partial_\eta$  does change the  $\eta$  dependence. But since  $\eta \sim \alpha_s\log\tau$  these terms are subleading to the dominant  $\alpha_s\log^2\tau$  and can get corrections from higher-loop effects. For example, at two-loops, a term of the form  $\alpha_s^2\log^2\tau$  is generated. Thus, SCET and CTTW agree to first order in  $\alpha_s$  and for the resummation of the leading large logarithms, which is the order to we have been working.

#### IV. MATCHING TO HARD EMISSIONS

Now let us look at how fixed order results and resummation are combined. There are two elements to this: (1) matching to hard emissions to get the differential distribution correct away from the two-jet region (i.e. away from  $\tau = 0$ ); and (2) including finite parts of loops to reproduce fixed order inclusive results.

Let us begin with the matching procedure described in [16]. To match to the hard emissions at order  $\alpha_s$  we need the parton model differential cross section from Eq. (7). The divergent part is already contained in the two-jet contribution, so the remainder is

$$\begin{aligned}
 D_{\text{fin}}(\tau) &= \int_0^\tau d\tau' d_{\text{fin}}(\tau') \\
 &= \log\tau[6\tau + 4\log(1-\tau)] - 2\log^2(1-\tau) + 3(1-2\tau)\log(1-2\tau) - 4\text{Li}_2\left(\frac{\tau}{1-\tau}\right) + 6\tau + \frac{9}{2}\tau^2. \quad (61)
 \end{aligned}$$

The final result for the matched integrated thrust distribution from [16] is

$$\left[\frac{1}{\sigma_0}R(\tau)\right]_{\text{CTTW}} = (1 + \sigma_1) \left\{ (1 + C_1) \exp[-2\bar{\alpha}\log^2\tau - 3\bar{\alpha}\log\tau] \frac{e^{-2\gamma_E\eta}}{\Gamma[2\eta + 1]} + \bar{\alpha}D_{\text{fin}}(\tau) \right\}, \quad (62)$$

where  $\sigma_1 = \frac{3}{2}\bar{\alpha} = \frac{\alpha_s}{\pi}$  is the NLO contribution to the total cross section and  $C_1 = \bar{\alpha}(\frac{\pi^2}{3} - \frac{5}{2})$  is chosen so that  $R(\frac{1}{3}) = 1 + \sigma_1$  (recall that  $\tau < \frac{1}{3}$  at order  $\alpha_s$ ). In the QCD approach the factor  $\sigma_1 = \frac{\alpha_s}{\pi}$  must be determined by a independent calculation of the total rate. This involves combining the real and virtual contributions at order  $\alpha_s$  using an appropriate infrared regulator. As emphasized in [16] there is arbitrariness in the matching because the hard emissions [in  $D_{\text{fin}}(\tau)$ ] are fixed order but the two-jet contribution is resummed. For example, to the same accuracy  $D(\tau)$  could be multiplied by the exponential.

Now, let us turn to the matching in SCET. To include thrust distributions away from the endpoint, we can either attempt to add power corrections to SCET, or we can match to higher order operators as described in [13,14]. Matching is much simpler. To perform the matching, we add new operators

$$\mathcal{O}_3 = \bar{\xi}_{n_1} A_{n_2}^\nu \gamma^\mu \xi_{n_3} + \dots, \quad (63)$$

where the  $\dots$  are the additional terms coming from Wilson lines necessary for gauge invariance.  $A_{n_2}^\mu$  is a collinear gluon in direction  $n_2$ . The matching demands that

$$\langle \mathcal{O}_2 \rangle_{\mu_h} + \langle \mathcal{O}_3 \rangle_{\mu_h} = \langle \text{QCD} \rangle_{\mu_h}, \quad (64)$$

where the subscript means the matching is done at the hard scale  $\mu_h$ .

There is some arbitrariness in the definition of the matrix elements in SCET due to reparametrization invariance. The matrix element of a collinear quark  $\xi_n(p)$  on a QCD quark state  $|q\rangle$  is only defined up to its soft momentum component  $n \cdot p$ . Moreover, a basis for summing over directions  $n$  for  $\mathcal{O}_2$  and  $n_1, n_2$ , and  $n_3$  for  $\mathcal{O}_3$  must be chosen as well. A certain convention was described in [13] for resolving these ambiguities and others are possible. In any case, while different conventions may shift the contributions from  $\mathcal{O}_2$  and  $\mathcal{O}_3$  in (64), the sum is parametrization invariant. Thus, independently of the convention we have

$$[d\sigma]_{\text{SCET}}^{\mu_h} = [d\sigma]_{\text{parton}}, \quad (65)$$

where  $[d\sigma]_{\text{parton}} \sim \langle \text{QCD} \rangle^2$  is the tree-level parton model cross section, as shown in Eq. (3).

Now, we already know that  $\langle \mathcal{O}_2 \rangle^2$  gives (50) to first order in  $\alpha_s$  and that the parton model distribution at order  $\alpha_s$  is (7). Thus, with obvious implicit phase space factors,

$$\langle \mathcal{O}_2 + \mathcal{O}_3 \rangle_{\mu_h}^2 - \langle \mathcal{O}_2 \rangle_{\mu_h}^2 = d_{\text{fin}}. \quad (66)$$

So, at leading order, the contribution from the sum of  $\langle \mathcal{O}_3 \rangle^2$  and the interference between  $\mathcal{O}_2$  and  $\mathcal{O}_3$  to the differential cross section is unambiguous. The running of  $\mathcal{O}_3$  could also be included even though it does not resum any large logs for the event shapes under consideration. With running, the matrix elements of  $\mathcal{O}_2$  and  $\mathcal{O}_3$  would appear with separate renormalization kernels, and so the final differential cross section would end up depending on the conventions chosen. The ambiguity could be resolved by a careful higher order treatment, but for the purposes of comparing to the CTTW prediction for thrust, we will simply not renormalize the finite terms.

Then,

$$\begin{aligned}
 \left[\frac{1}{\sigma_0}R(\tau)\right]_{\text{SCET}} &= \exp[-2\bar{\alpha}\log^2\tau - 3\bar{\alpha}\log\tau] \tilde{r}(\partial_\eta) \\
 &\quad \times \frac{e^{-2\gamma_E\eta}}{\Gamma[1+2\eta]} + \bar{\alpha}D_{\text{fin}}(\tau). \quad (67)
 \end{aligned}$$

With  $\tilde{r}(\partial_\eta)$  and  $\eta$  as in Eq. (60) and  $D_{\text{fin}}(\tau)$  in (61). The total cross section in SCET is given

$$\begin{aligned}
 \left[R\left(\frac{1}{3}\right)\right]_{\text{SCET}} &= \sigma_0 \left[ 1 + \bar{\alpha} \left( -1 + \frac{\pi^2}{3} \right) + \bar{\alpha} D_{\text{fin}}\left(\frac{1}{3}\right) \right] \\
 &= \sigma_0 \left[ 1 + \frac{\alpha_s}{\pi} \right]. \quad (68)
 \end{aligned}$$

This is the correct total  $e^+e^-$  total cross section to first order in  $\alpha_s$ !

Let us review the contributions that go into the cross section. First, at the hard scale  $\mu_h = Q$ , there is the finite part of the loop matching to QCD,  $|c_H|^2 = 1 + \bar{\alpha}(-8 + \frac{7\pi^2}{6}) = 1 + 2.3\sigma_1$ . Next, at the scale  $\mu_j^2 = p^2 = Q^2\tau$  where we integrate out the collinear fields, the jet functions give  $2c_J = \bar{\alpha}(7 - \pi^2) = -1.9\sigma_1$ . At the seesaw scale  $\mu_s = p^2/Q$ , the soft function gives  $2c_S = \frac{\pi^2}{6} = 1.1\sigma_1$ , and finally the finite part of the real emission integral, away from  $\tau = 0$  gives  $\sigma_3 = \bar{\alpha}(\frac{5}{2} - \frac{\pi^2}{3}) = -0.5\sigma_1$ . In producing the total cross section, only the soft and jet contributions are infrared divergent. However, their convolution, which appears in the function  $K(p^2, \mu)$  is infrared finite. The hard matching and the hard emissions are IR finite by themselves. Thus, the total cross section can be understood as a combination of a process dependent



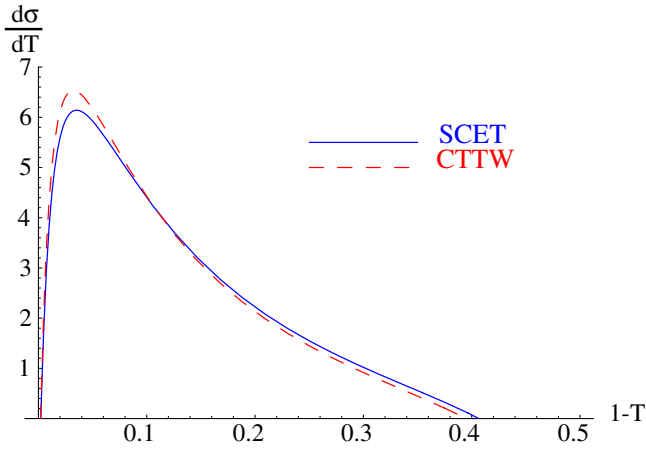


FIG. 1 (color online). Matched resummed differential thrust distribution in SCET and in the standard approach of CTTW with fixed coupling  $\alpha_s = 0.4$ .

IR finite hard part and universal but IR regulator dependent contributions from soft and collinear emissions.

The SCET thrust distribution (67) is compared to the CTTW thrust distribution (62) in Fig. 1. The plot is of  $\frac{d\sigma}{dT} = R'(\tau)$  with  $\alpha_s$  fixed at 0.4. A more careful rendition of the differential thrust distribution would take the derivative of  $R(\tau)$  before assigning the matching scale  $\mu_j = Q\sqrt{\tau}$ , as is done below. However, the effect is higher order, and so we just plot  $R'(\tau)$  directly.

## V. GENERALIZATIONS

In this section, some simple generalizations are described. The above results were derived assuming  $\alpha_s$  to be constant in order to emphasize the resummation of Sudakov logarithms in contrast to large logarithms associated with the scale  $\Lambda_{\text{QCD}}$ . Now, it is shown how the results can be modified with running  $\alpha_s$ . Also, the SCET prediction for another event shape, the jet mass  $\rho$ , is given.

It is straightforward to allow  $\alpha_s$  to run. Including 1-loop running, the effect is to modify the single and double logs in the following way [11]:

$$\begin{aligned} \bar{\alpha} \log^2 \frac{\mu}{\nu} &\rightarrow -S(\nu, \mu) \\ &= -\frac{4\pi C_F}{\beta_0^2 \alpha_s(\nu)} \left[ 1 - \frac{\alpha_s(\nu)}{\alpha_s(\mu)} - \log \frac{\alpha_s(\mu)}{\alpha_s(\nu)} \right] \end{aligned} \quad (69)$$

$$\bar{\alpha} \log \frac{\mu}{\nu} \rightarrow -A(\nu, \mu) = -\frac{C_F}{\beta_0} \log \frac{\alpha_s(\mu)}{\alpha_s(\nu)}. \quad (70)$$

For example, the differential thrust distribution for  $\tau > 0$  with running  $\alpha_s$  becomes

$$\begin{aligned} \left[ \frac{1}{\sigma_0} \frac{d\sigma}{d\tau} \right]_{\text{SCET}} &= \frac{1}{\tau} \exp[4S(Q, Q\tau) + 6A(Q, Q\tau) \\ &\quad - 8S(Q\sqrt{\tau}, Q\tau) - 6A(Q\sqrt{\tau}, Q\tau)] \bar{r}(\partial_\eta) \\ &\quad \times \frac{e^{-2\gamma_E \eta}}{\Gamma[2\eta]} + \frac{2\alpha_s}{3\pi} d_{\text{fin}}(\tau), \end{aligned} \quad (71)$$

where

$$\eta = 4A(Q\sqrt{\tau}, Q), \quad (72)$$

$d_{\text{fin}}$  is given in Eq. (7) and

$$\begin{aligned} \bar{r}(\partial_\eta) &= 1 + \frac{2}{3\pi} \left\{ \left( -8 + \frac{7\pi^2}{6} \right) \alpha_s(Q) + \left( 7 - \frac{2\pi^2}{3} \right) \alpha_s(Q\sqrt{\tau}) \right. \\ &\quad - \frac{\pi^2}{2} \alpha_s(Q\tau) + \left[ \frac{1}{2} \alpha_s(Q\sqrt{\tau}) - \alpha_s(Q\tau) \right] \partial_\eta^2 \\ &\quad \left. - \frac{3}{2} \alpha_s(Q\sqrt{\tau}) \partial_\eta \right\}. \end{aligned} \quad (73)$$

This is the same function  $\bar{r}$  as in Eq. (60), but with the  $\alpha_s$  factors evaluated at the appropriate matching scales.

At this point, one would hope to compare to data. However, besides the obvious shortcoming of not containing the full NLL resummation (it does not include effects of the two-loop cusp anomalous dimension), this parton-level expression does not include important nonperturbative effects. Because of the running of  $\alpha_s$ , the perturbative expression breaks down when the soft scale is of order  $\Lambda_{\text{QCD}}$ , that is, when  $\tau \sim \Lambda_{\text{QCD}}/Q$ , as can be seen explicitly in (73). In fact, even for significantly larger values of thrust power corrections of order  $\Lambda_{\text{QCD}}/Q$  become quantitatively important, at least at LEP energies. This problem has been approached elsewhere using SCET [25,26] and with other techniques [21,29,30].

Other event shapes can be studied the same way as thrust. For example, consider the heavy jet mass  $\rho$  defined by

$$\rho \equiv \frac{1}{Q^2} \max(p_L^2, p_R^2). \quad (74)$$

In this case, the matching scales are  $\mu_h = Q$ ,  $\mu_j = Q\sqrt{\rho}$ , and  $\mu_s = Q\rho$  and SCET gives for  $\rho > 0$

$$\begin{aligned} \left[ \frac{1}{\sigma_0} \frac{d\sigma}{d\rho} \right]_{\text{SCET}} &= \frac{2}{\rho} |1 + c_H|^2 \exp[4S(Q, Q\rho) \\ &\quad + 6A(Q, Q\rho) - 8S(Q\sqrt{\rho}, Q\rho) \\ &\quad - 6A(Q\sqrt{\rho}, Q\rho)] \left[ \tilde{k}(\partial_\eta) \frac{e^{-\gamma_E \eta}}{\Gamma[\eta]} \right] \\ &\quad \times \left[ \tilde{k}(\partial_\eta) \frac{e^{-\gamma_E \eta}}{\Gamma[\eta + 1]} \right] + \frac{2\alpha_s}{3\pi} d_{\text{fin}}(\rho), \end{aligned} \quad (75)$$

where

$$\eta = 4A(Q\sqrt{\rho}, Q). \quad (76)$$

This formula agrees with the jet mass distribution in [16] to leading log and first order in  $\alpha_s$ . The same function  $d_{\text{fin}}$  appears for jet mass and for thrust because to order  $\alpha_s$  in the parton model,  $\rho = \tau = \frac{1}{Q^2} \min(s, t, u)$ .

## VI. CONCLUSIONS

We have investigated how to combine resummation with next-to-leading order matching of event shapes in the original approach of [18] (CTTW) and using SCET. In the CTTW formulation, real emissions from collinear splitting functions are used and various kinematical features associated with soft emission are combined to derive a differential cross section. The cross section factorizes into the product of two jet functions. Resummation is done by solving a differential equation for the jet functions in terms of the physical scales  $p^2$  and  $Q^2$  of the event. In contrast, SCET factorizes the event shape distribution into a contribution from hard, jet, and soft functions. These functions are matched at the scales  $\mu_h = Q$ ,  $\mu_j = p$  and  $\mu_s = \frac{p^2}{Q}$  respectively and resummation is done through renormalization group evolution. The resummed thrust distribution in SCET and CTTW have been compared, and found to agree to next-to-leading order in  $\alpha_s$  and for leading-log resummation.

The resummation of thrust in SCET brings to light a number of features of the process not obvious in CTTW formulation. For example, the appearance of the seesaw scale  $\mu_s = Q(1 - T)$  as the natural matching scale for the soft function follows from the kinematics of the SCET factorization theorem. Of course, the existence of this scale has been known for a long time from QCD, but in the effective field theory approach this scale just drops out of the factorized expression. Thus, for more complicated processes, it is reasonable to expect a similar transparency for the matching scales, which may facilitate subleading log resummation. In fact, two-loop, three-loop, and some

four-loop anomalous dimensions for various quantities are already available [27,32–34], and so subleading log resummation appears quite feasible. The biggest impediment to using these more accurate resummed results in a comparison to data is that power corrections of order  $\Lambda_{\text{QCD}}/Q$  have an important quantitative effect on event shapes. However, these corrections should modify only the soft function while higher order resummed expressions for the hard and jet functions will remain valid. Thus, the effective theory should be able to weave together the perturbative and nonperturbative calculations.

A new result of this paper is the demonstration that inclusive quantities, such as the total cross section for  $e^+e^-$  can be calculated in a new way using SCET. Instead of taking the full differential  $n + 1$  body cross section and combining with the one-loop  $n$ -body cross section, SCET combines finite parts of loops of soft and jet functions with a hard matching calculation and a finite integral over hard emissions. The soft and jet functions depend on the infrared regulator, but their convolution, and the hard function, do not. For  $e^+e^-$  annihilation at NLO, this may not be so impressive, but the procedure promises to apply to more complicated processes, perhaps even some for which NLO results are not available. It would also be very interesting to explore this mechanism at NNLO or to work with hadronic processes where the singularity structure is more complicated.

## ACKNOWLEDGMENTS

I would like to thank T. Becher and S. Fleming for many useful discussions. I also benefited from the hospitality of the Les Houches Ecole de Physique and discussions with many of its participants. This work was supported in part by the National Science Foundation under grant NSF-PHY-0401513 and by the Johns Hopkins Theoretical Interdisciplinary Physics and Astronomy Center.

- 
- [1] C. W. Bauer, S. Fleming, and M. E. Luke, Phys. Rev. D **63**, 014006 (2000).
  - [2] C. W. Bauer, S. Fleming, D. Pirjol, and I. W. Stewart, Phys. Rev. D **63**, 114020 (2001).
  - [3] C. W. Bauer, D. Pirjol, and I. W. Stewart, Phys. Rev. D **65**, 054022 (2002).
  - [4] M. Beneke, A. P. Chapovsky, M. Diehl, and T. Feldmann, Nucl. Phys. **B643**, 431 (2002).
  - [5] C. W. Bauer, S. Fleming, D. Pirjol, I. Z. Rothstein, and I. W. Stewart, Phys. Rev. D **66**, 014017 (2002).
  - [6] C. W. Bauer and A. V. Manohar, Phys. Rev. D **70**, 034024 (2004).
  - [7] S. W. Bosch, B. O. Lange, M. Neubert, and G. Paz, Nucl. Phys. **B699**, 335 (2004).
  - [8] M. Neubert, Eur. Phys. J. C **40**, 165 (2005).
  - [9] A. V. Manohar, Phys. Rev. D **68**, 114019 (2003).
  - [10] T. Becher and M. Neubert, Phys. Rev. Lett. **97**, 082001 (2006).
  - [11] T. Becher, M. Neubert, and B. D. Pecjak, J. High Energy Phys. **01** (2007) 076.
  - [12] S. Fleming, A. H. Hoang, S. Mantry, and I. W. Stewart, arXiv:hep-ph/0703207.
  - [13] C. W. Bauer and M. D. Schwartz, Phys. Rev. D **76**, 074004 (2007).
  - [14] C. W. Bauer and M. D. Schwartz, Phys. Rev. Lett. **97**, 142001 (2006).
  - [15] M. Trott, Phys. Rev. D **75**, 054011 (2007).
  - [16] S. Catani, L. Trentadue, G. Turnock, and B. R. Webber,

- Nucl. Phys. **B407**, 3 (1993).
- [17] S. Catani, G. Turnock, B. R. Webber, and L. Trentadue, Phys. Lett. B **263**, 491 (1991).
- [18] S. Catani, M. L. Mangano, P. Nason, and L. Trentadue, Nucl. Phys. **B478**, 273 (1996).
- [19] Y. L. Dokshitzer, A. Lucenti, G. Marchesini, and G. P. Salam, J. High Energy Phys. 01 (1998) 011.
- [20] N. Kidonakis, G. Oderda, and G. Sterman, Nucl. Phys. **B525**, 299 (1998).
- [21] E. Gardi and J. Rathsmann, Nucl. Phys. **B609**, 123 (2001).
- [22] C. F. Berger, T. Kucs, and G. Sterman, Phys. Rev. D **68**, 014012 (2003).
- [23] S. Catani, B. R. Webber, and G. Marchesini, Nucl. Phys. **B349**, 635 (1991).
- [24] S. Catani and M. H. Seymour, Nucl. Phys. **B485**, 291 (1997); **B510**, 503(E) (1998).
- [25] C. W. Bauer, A. V. Manohar, and M. B. Wise, Phys. Rev. Lett. **91**, 122001 (2003).
- [26] C. Lee and G. Sterman, Phys. Rev. D **75**, 014022 (2007).
- [27] T. Becher and M. Neubert, Phys. Lett. B **637**, 251 (2006).
- [28] G. P. Korchemsky and G. Marchesini, Phys. Lett. B **313**, 433 (1993).
- [29] G. P. Korchemsky and S. Tafat, J. High Energy Phys. 10 (2000) 010.
- [30] G. P. Korchemsky and G. Sterman, Nucl. Phys. **B555**, 335 (1999).
- [31] G. P. Korchemsky and A. V. Radyushkin, Nucl. Phys. **B283**, 342 (1987).
- [32] A. V. Belitsky, Phys. Lett. B **442**, 307 (1998).
- [33] S. Moch, J. A. M. Vermaseren, and A. Vogt, Nucl. Phys. **B688**, 101 (2004).
- [34] T. Becher and M. Neubert, Phys. Lett. B **633**, 739 (2006).